ELSEVIER

Carbohydrate Research 295 (1996) 127–146

CARBOHYDRATE RESEARCH

The structures of oligosaccharides isolated from the lipopolysaccharide of *Moraxella catarrhalis* serotype B, strain CCUG 3292

Per Edebrink [a], Per-Erik Jansson [b,*], Göran Widmalm [a], Tord Holme [c], Motiur Rahman [c]

[a] *Department of Organic Chemistry, Arrhenius Laboratory, Stockholm University, S-106 91 Stockholm, Sweden*

[b] *Clinical Research Centre, Analytical Unit, Karolinska Institute, Huddinge Hospital, NOVUM, S-141 86 Huddinge, Sweden*

[c] *Microbiology and Tumor Biology Centre, Division of Bacteriology, Karolinska Institute, S-171 77 Stockholm, Sweden*

Received 3 June 1996; accepted 20 August 1996

Abstract

The oligosaccharides from the lipopolysaccharides of *Moraxella catarrhalis* serotype B, strain CCUG 3292, were isolated after mild acid hydrolysis and separated by high-performance anion-exchange chromatography. The structures of the oligosaccharides were established by fast atom bombardment mass spectrometry and nuclear magnetic resonance spectroscopy. It is concluded that the oligosaccharides comprise a mixture of mainly a nona- and a deca-saccharide.

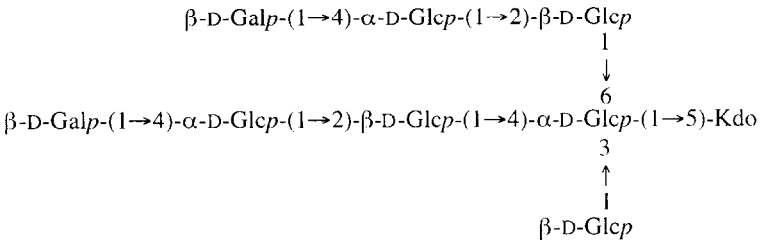

* Corresponding author. Tel.: +46-8-7465204. Fax: +46-8-7465230. E-mail: Pererik.Jansson@kfcm13.hs.sll.se.

PII S0008-6215(96)00218-2

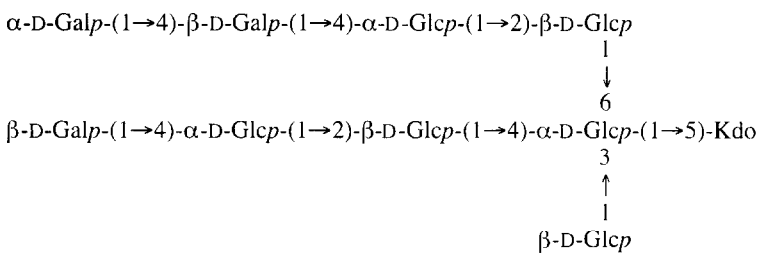

Smaller amounts of undecasaccharides and of truncated forms, namely, hexa-, hepta-, and octa-saccharides, were also detected. © 1996 Elsevier Science Ltd.

Keywords: *Moraxella catarrhalis*; *Branhamella*; Lipopolysaccharide; NMR

1. Introduction

Moraxella catarrhalis is a common cause of otitis media and sinusitis in children [1,2]. It is also a significant pathogen causing bronchitis and pneumonia in adults who are immunocompromised or who have predisposing conditions, such as chronic bronchitis or chronic obstructive pulmonary disease [3]. The lipopolysaccharide (LPS) of *M. catarrhalis* does not possess the extended side chains carrying the O-antigenic determinants characteristic of the LPSs from enteric bacteria [4]. It is, however, toxic to experimental animals, and is probably contributing to the virulence of *M. catarrhalis* [5]. Serological typing of *M. catarrhalis* LPSs using hyperimmune rabbit sera has shown the existence of three major serotypes: A (60%), B (30%), and C (5%), thus accounting for approximately 95% of isolates from patients [6]. Cross-reactions between serotypes have been described indicating the presence of common epitopes [6]. We and others have recently reported the structures of the oligosaccharide portion of *M. catarrhalis* LPSs from one type A strain [7–9] and two type C strains [10]. Structure **1** was concluded for the oligosaccharide of type A and structures **2–5** for type C. For both serotypes, a second Kdo residue was linked to the 4-position of the 5-substituted Kdo residue shown in the structure. In type A, lipid A was of the conventional type with a β-linked glucosamine disaccharide acylated at the two nitrogens and at position three of both residues with C-10 and C-12 acids [7]. Phosphates were present at C-1 and C-4′. In this paper we report structural studies of the oligosaccharide part of the LPS from a type B strain.

2. Results and discussion

LPS was prepared from cells of *M. catarrhalis* serotype B, strain CCUG 3292 as described earlier [8]. Treatment of the LPS in 0.1 M acetate buffer of pH 4.4, containing 0.1% sodium dodecyl sulfate, for 2 h at 100 °C yielded after further treatment a

lipid-free solution of the oligosaccharides. These were purified by gel permeation chromatography on a Superdex 30 column where they were eluted in the region for large oligosaccharides. Pseudomolecular ions, $[M-H]^-$, were observed at *m/z* 1047.3, 1209.5, 1371.5, 1533.7, 1695.7, and 1858.4 in the FAB mass spectrum of the oligosaccharide fraction. The pseudomolecular ions correspond to oligosaccharides with the formula Hex_nKdo, where the number of hexosyl residues *n* can take any value from five to ten. The oligosaccharides were designated OS(6), OS(7), OS(8), OS(9), OS(10), and OS(11), the number in parenthesis referring to the number of sugar residues in each oligosaccharide. A hydrolysate of the oligosaccharide mixture contained glucose and galactose in the ratio 7:3; other sugars were not detected in significant amounts. On biosynthetic grounds the absolute configurations were assumed to be the same as before, that is, D. From NMR data, see below, it was evident that all sugar residues were pyranoid. Methylation analysis data of the oligosaccharide mixture showed the presence of gluco- and galacto-pyranosyl end groups, 2-substituted glucopyranosyl residues, 4-substituted gluco- and galacto-pyranosyl residues, and 3,4,6-trisubstituted glucopyranosyl residues. Thus, serotype B is devoid of 2-acetamido-2-deoxyglucopyranosyl residues which are present in serotypes A and C.

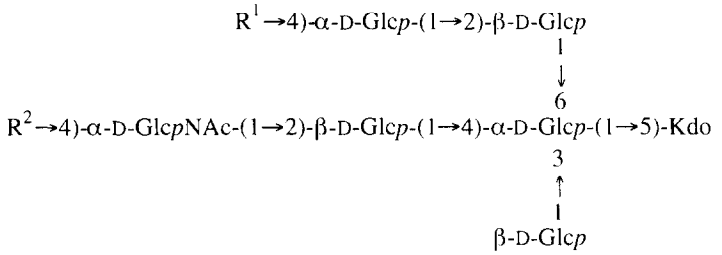

1 R^1 = α-D-Gal*p*-(1→4)-β-D-Gal*p*-(1→
R^2 = H

2 R^1 = H
R^2 = H

3 R^1 = H
R^2 = β-D-Gal*p*-(1→

4 R^1 = α-D-Gal*p*-(1→4)-β-D-Gal*p*-(1→
R^2 = β-D-Gal*p*-(1→

5 R^1 = α-D-Gal*p*-(1→4)-β-D-Gal*p*-(1→
R^2 = α-D-Gal*p*-(1→4)-β-D-Gal*p*-(1→

Table 1
NMR chemical shifts for the oligosaccharides from *M. catarrhalis* serotype B (strain CCUG 3292)

Residue [a]	Glycose unit [b]	Atom [c]	Chemical shifts (δ) [d]					
			OS(6)	OS(7)	OS(9)		OS(10)	
			^{1}H	^{1}H	^{1}H	^{13}C	^{1}H	^{13}C
A	→ 3,4,6)-α-D-Glc*p*-(1 →	1	5.16	5.16	5.15	100.3	5.16	100.4
			[4.1] [e]	[4.2]	[3.7]		[3.7]	
		2	3.86	3.90	3.89	73.8	3.89	73.8
		3	4.39	4.43	4.44	76.4	4.45	76.4
		4	3.94	4.04	4.03	74.5	4.03	74.5
		5	4.53	4.61	4.63	70.7	4.63	70.6
		6a	4.21	4.04	4.04	68.7	4.05	68.7
		6b	4.03	4.18	4.17		4.18	
B	β-D-Glc*p*-(1 →	1	4.99	4.95	4.96	103.4	4.96	103.5
			[7.9]	[7.8]	[7.6]		[7.0]	
		2	3.38	3.41	3.44	74.2	3.44	74.2
		3	3.54	3.54	3.53	76.6	3.52	76.7
		4	3.43	3.40	3.40	70.5	3.42	70.5
		5	3.50	3.51	3.50	76.6	3.49	76.4
C	→ 2)-β-D-Glc*p*-(1 →	1	4.73	5.11	5.12	98.9	5.12	99.0
			[7.8]	[7.9]	[7.3]		[7.0]	
		2	3.35	3.45	3.44	80.4	3.44	80.4
		3	3.52	3.62	3.62	75.4	3.63	75.4
		4		3.44	3.44	70.4	3.44	70.5
		5		3.48	3.48	76.5	3.48	76.5
D	→ 2)-β-D-Glc*p*-(1 →	1	4.64	4.65	4.65	103.6	4.65	103.7
			[7.7]	[8.0]	[7.6]		[7.4]	
		2	3.48	3.48	3.48	77.4	3.49	77.2
		3	3.59	3.58	3.58	75.4	3.59	75.4
		4		3.44	3.42	70.5	3.43	70.5
		5		3.46	3.45	76.6	3.46	76.9
E	→ 4)-α-D-Glc*p*-(1 →	1	5.44	5.45	5.44	97.7	5.46	97.7
			[3.8]	[3.9]	[4.0]		[4.0]	
		2	3.57	3.58	3.66	71.9	3.66	71.9
		3	3.76	3.77	3.88	72.4	3.88	72.6
		4	3.46	3.46	3.69	79.1	3.70	79.3
		5	~ 4.02	~ 4.02	4.13	71.2	4.13	71.3
F	→ 4)-α-D-Glc*p*-(1 →	1		5.30	5.28	99.4	5.28	99.4
				[3.8]	[3.6]		[3.6]	
		2		3.50	3.56	71.9	3.56	72.1
		3		3.72	3.88	72.8	3.88	72.6
		4		3.48	3.70	79.1	3.71	79.1
		5		~ 4.01	4.12	71.3	4.12	71.3
G	β-D-Gal*p*-(1 →	1			4.47	103.9	4.48	103.9
					[7.6]		[7.6]	
		2			3.55	71.8	3.56	71.9
		3			3.68	73.4	3.68	73.4
		4			3.93	69.4	3.94	69.4
		5			3.74	76.2	3.75	76.2

Table 1 (continued)

Residue [a]	Glycose unit [b]	Atom [c]	Chemical shifts (δ) [d]					
			OS(6)	OS(7)	OS(9)		OS(10)	
			^{1}H	^{1}H	^{1}H	^{13}C	^{1}H	^{13}C
H	→4)-β-D-Gal*p*-(1→	1			4.47 [7.6]	103.9	4.54 [7.9]	104.2
		2			3.55	71.8	3.59	71.8
		3			3.68	73.4	3.76	73.1
		4			3.93	69.4	4.06	78.2
		5			3.74	76.2	3.80	76.3
I	α-D-Gal*p*-(1→	1					4.96 [4.3]	101.3
		2					3.85	69.4
		3					3.92	70.0
		4					4.05	69.8
		5					4.37	71.7
		6					3.72	61.4
K	→5)-α-Kdo*p*	3ax					2.04	34.9
		3eq					1.88	
		4	4.15	4.15	4.15	66.7	4.15	66.6
		5	4.08	4.08	4.08	76.1	4.09	76.1
		6			3.84	72.2	3.85	72.2
		7			4.05	69.2	4.06	69.4
		8a			3.63	63.9	3.64	63.9
		8b			3.81		3.81	

[a] Residue designations are in accord with the text.
[b] Glycose units are given as they appear in OS(10).
[c] Numerals refer to protons.
[d] ^{1}H NMR chemical shifts at 25 °C are given relative to TSP (δ 0.00). ^{13}C NMR chemical shifts at 25 °C are given relative to dioxane (δ 67.4).
[e] $J_{H\text{-}1,H\text{-}2}$ values [Hz] are given within square brackets.

The oligosaccharides were fractionated by high-performance anion-exchange chromatography and collected in four fractions. Desalting by gel permeation chromatography yielded four oligosaccharide preparations **f1** (~ 10%), **f2** (~ 40%), **f3** (~ 40%), and **f4** (~ 10%). FABMS analysis showed **f1** to contain OS(6) and OS(7) as the major components, and that **f2** and **f3** contained mainly OS(9) and OS(10), respectively. Small amounts of OS(8) were present in **f1** and **f2**. The FABMS analysis indicated **f4** to contain only OS(11).

The ^{1}H NMR spectra of the oligosaccharide preparations were devoid of signals for *N*-acetyl groups, thus further substantiating the absence of 2-acetamido-2-deoxyglucosyl residues in the oligosaccharides. The $J_{H\text{-}1,H\text{-}2}$ values, which were extracted directly from the one-dimensional ^{1}H NMR spectra or, in the case of overlapping signals, from the ^{1}H,^{1}H COSY spectra, demonstrated the anomeric configuration of the glucosyl and galactosyl residues (Table 1). The reducing Kdo residues had the α configuration as

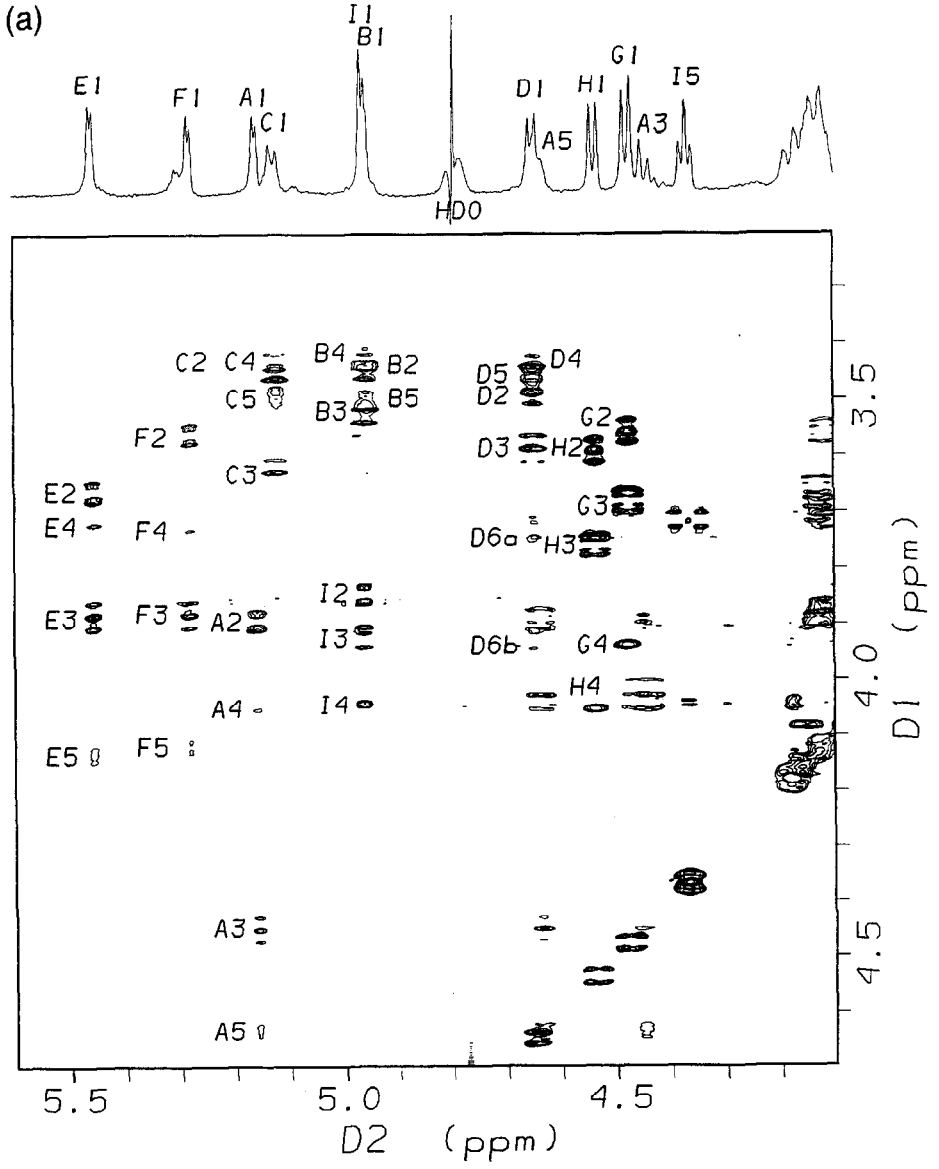

Fig. 1. (a) Section of a phase-sensitive 2D HOHAHA NMR spectrum of OS(10) with a spin-lock time of 90 ms recorded at 400 MHz and 25 °C. Cross-peaks are annotated along the D2 axis with residue designations and atom numbers. (b) Section of a phase-sensitive 2D NOESY spectrum of OS(10) with a mixing time of 350 ms recorded at 400 MHz and 25 °C. Cross-peaks are annotated along the D1 axis with residue designations and atom numbers.

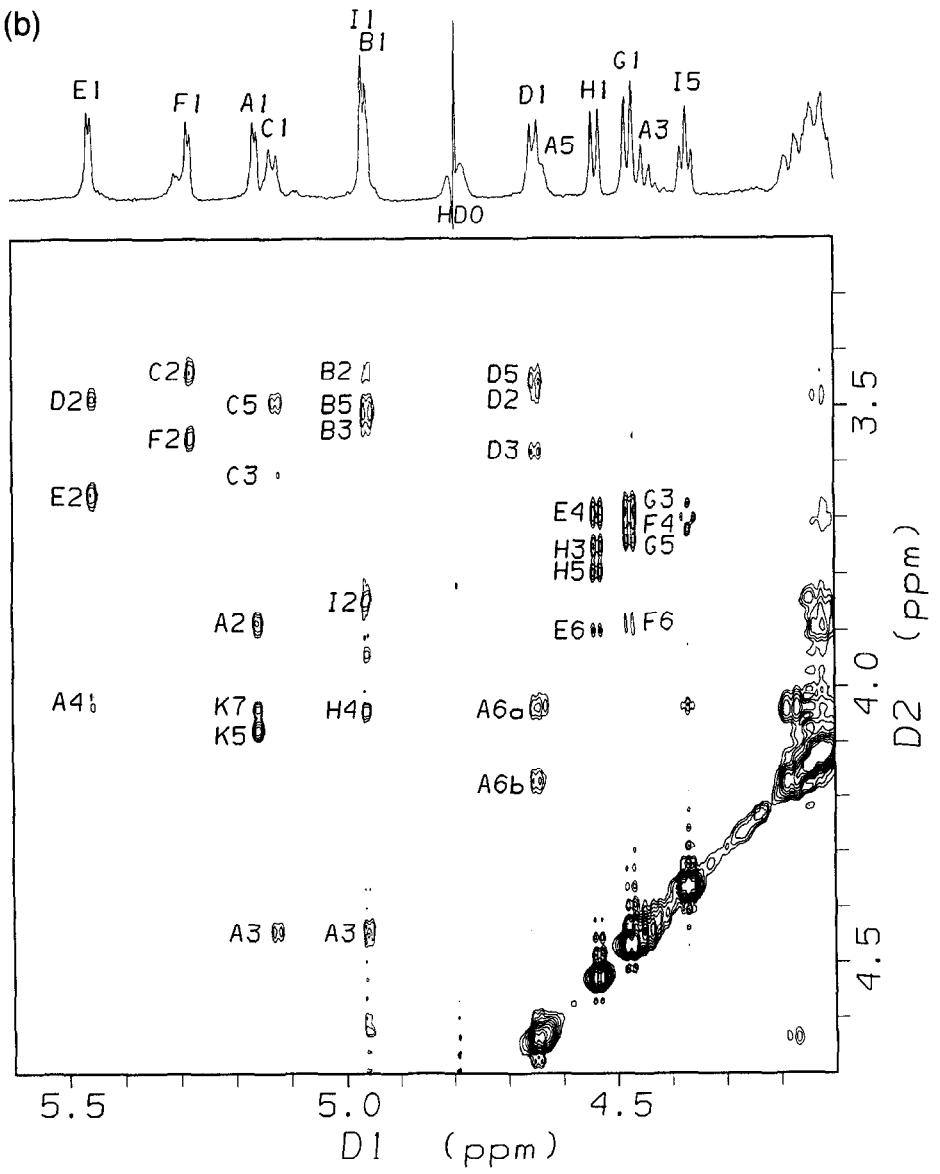

Fig. 1 (continued).

evident from the chemical shift values of the signals of the 3-deoxy protons [8]. The observed $^{3}J_{H,H}$ values indicated that all the hexosyl residues were pyranoid and existed in the $^{4}C_{1}$ conformation. The signals in the ^{1}H NMR spectra of OS(9), OS(10), and OS(11) were assigned from $^{1}H,^{1}H$-correlated DQF COSY (double quantum filtered

correlated spectroscopy) and HOHAHA (homonuclear Hartman–Hahn) spectra (Table 1). The ^{13}C NMR signals of OS(9) and OS(10) were assigned from ^{1}H-detected HMQC (heteronuclear multiple quantum coherence), HSQC (heteronuclear single quantum coherence), and HSQC-HOHAHA (heteronuclear single quantum coherence HOHAHA) spectra (Table 1).

Structure of OS(10).—Signals for nine anomeric protons and three ring protons were observed in the region δ 4.2–5.6 of the ^{1}H NMR spectrum of OS(10). The hexosyl residues were designated **A**–**I**. From ^{13}C glycosylation shifts and $^{1}H,^{1}H$ couplings the residues could be assigned as follows. Residue **A** ($\delta_{H\text{-}1}$ 5.16) was assigned to a 3,4,6-trisubstituted α-D-glucopyranosyl residue and residue **B** ($\delta_{H\text{-}1}$ 4.96) to a β-D-glucopyranosyl group. Residues **C** and **D** ($\delta_{H\text{-}1}$ 5.12 and 4.65, respectively) were assigned to two 2-substituted β-D-glucopyranosyl residues, **E** and **F** ($\delta_{H\text{-}1}$ 5.46 and 5.28, respectively) to two 4-substituted α-D-glucopyranosyl residues, **G** ($\delta_{H\text{-}1}$ 4.48) to a β-D-galactopyranosyl group, **H** ($\delta_{H\text{-}1}$ 4.54) to a 4-substituted β-D-galactopyranosyl residue, and **I** ($\delta_{H\text{-}1}$ 4.96) to an α-D-galactopyranosyl group. The Kdo residue, designated **K**, constitutes the reducing end of OS(10) and was shown to be 5-substituted.

Intra-residue NOE correlations that corroborated the anomeric configurations were observed in a NOESY spectrum, since correlations from anomeric protons in β-linked sugars were generally observed to either or both of H-3 and H-5. When considering the types of glycosidic linkage which can be formed from the glycosyl residues listed above, it is reasonable to assume that inter-residue correlations across the glycosidic linkage directly reflect the type of linkage. This assumption should be valid provided that the conformation of each constituent disaccharide element in the oligosaccharide is similar to that observed for the corresponding free disaccharide, per se. Thus, in agreement with this expectation, inter-residue $^{1}H-^{1}H$ NOE correlations that established one tetrasaccharide branch (**I-H-E-D**) and one trisaccharide branch (**G-F-C**) were observed in the NOESY spectrum, cf., the HOHAHA spectrum (Figs. 1a and b, respectively). Correlations between the anomeric proton and the proton on the linkage carbon were observed for all five disaccharide elements, **I-H** (δ 4.96–δ 4.06), **H-E** (δ 4.54–δ 3.70), **E-D** (δ 5.46–δ 3.49), **G-F** (δ 4.48–δ 3.71), and **F-C** (δ 5.28–δ 3.44). A long-range NOE correlation between H-1 of **E** and H-4 of **A**, which is the 3,4,6-trisubstituted α-D-glucopyranosyl residue (δ 4.03), was also observed. However, as **E** is embedded between **H** and **D** it cannot substitute **A**. Residue **D** was shown to substitute the primary position of the branch-point residue **A** from correlations between its anomeric proton and the hydroxymethyl protons (δ 4.05 and 4.18). The anomeric proton of residue **C** had two correlations to residue **A**, a medium one to H-4 (δ 4.03) and a strong one to H-3 (δ 4.45), but an NOE correlation between the anomeric proton of the β-D-glucopyranosyl group **B** and H-3 of **A** (δ 4.45) indicated that **B** substitutes the 3-position of the branch-point residue. From HMBC data, described below, it is clear that this is the substitution pattern of residue **A** in OS(10). Finally, an inter-residue NOE correlation between H-1 of residue **A** and H-5 of residue **K** (δ 4.09), the 5-substituted Kdo moiety, demonstrated a (1 → 5) linkage. A second correlation, of lower intensity, between H-1 of **A** and H-7 of **K** (δ 4.06) was also observed. Thus, structure **10** was concluded for OS(10).

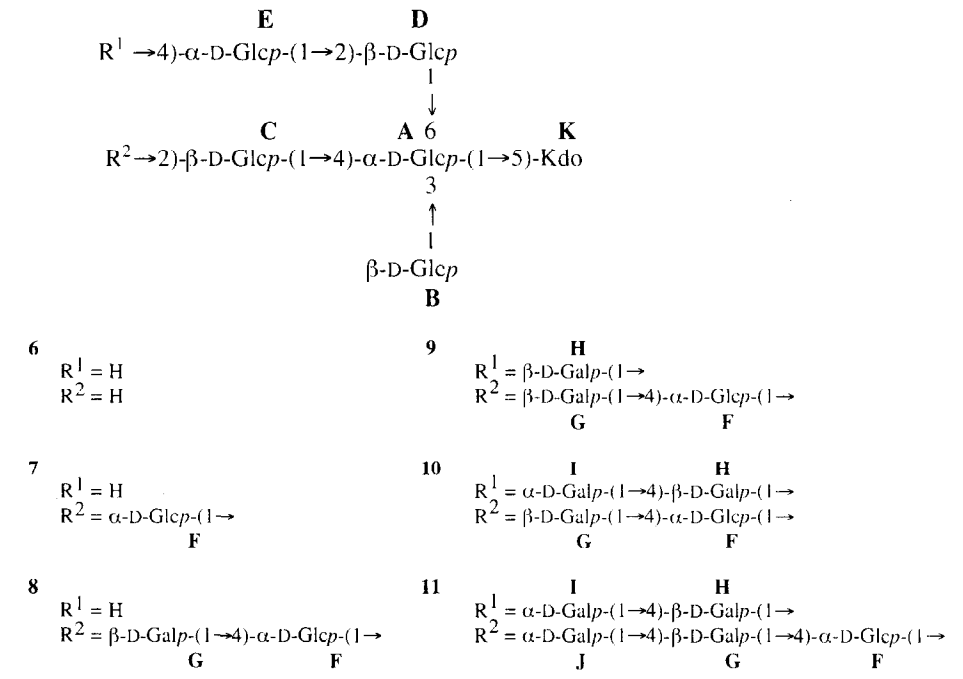

Multiple bond correlations were observed in an HMBC (heteronuclear multiple bond correlation) spectrum (Table 2). Intra-residual multiple bond correlations were valuable for confirmation of the assignments of signals for C-3 and C-5 of α-linked residues, and of signals for H-2 and H-5 of β-linked residues. Inter-residue three-bond heteronuclear correlations corroborated structure **10** from the following correlations. Residue **I** had three-bond correlations from H-1 and C-1 to C-4 and H-4, respectively, of residue **H**, which had the corresponding three-bond correlations to C-4 and H-4, respectively, of residue **E**. Residue **E** was linked to residue **D**, as demonstrated by an inter-residue correlation between C-1 of the former and H-2 of the latter. The anomeric proton of residue **D** had a correlation to C-6 of **A**, the branch-point residue. Residue **G** had three-bond correlations from H-1 and C-1 to both C-4 and H-4, respectively, of residue **F**, which had a correlation from C-1 to H-2 of residue **C**. The data from the NOESY experiment could not be interpreted unambiguously with respect to the substitution pattern of residue **A**. However, the HMBC spectrum demonstrated that residue **C** was substituting the 4-position of residue **A**, observed through a correlation between H-1 in **C** and C-4 in **A**. A correlation, δ_H 4.96–δ_C 76.4, is in accord with a (1 → 3) linkage between residues **B** and **A** since the signal for C-3 in **A** resonates at δ 76.4, but also with intra-residue correlations between H-1 in **B** and atoms C-3 (δ 76.7) and C-5 (δ 76.4). The latter interpretation is, however, less likely, since the $J_{H\text{-}1,C\text{-}3}$ and $J_{H\text{-}1,C\text{-}5}$ values for a β-D-glucopyranoside derivative have been reported to be small, 1.1 and 1.2 Hz, respectively. Further evidence that residue **B** substitutes the 3-position of residue **A** was obtained from an HMBC correlation between the anomeric carbon (δ_C 103.5) of residue **B** and H-3 in residue **A** (δ_H 4.45). Finally, C-1 in the branch-point residue, **A**,

Table 2
Summary of inter- and intra-residue correlations observed from anomeric nuclei in NOESY, ROESY, and HMBC NMR spectra of oligosaccharides from *M. catarrhalis* serotype B

I H E D
α-D-Gal*p*-(1→4)-β-D-Gal*p*-(1 → 4)-α-D-Glc*p*-(1→2)-β-D-Glc*p*-(1 → 6
G F C A K
β-D-Gal*p*-(1→4)-α-D-Glc*p*-(1 → 2)-β-D-Glc*p*-(1 → 4)-α-D-Glc*p*-(1→5)-α-Kdo*p*
B 3
β-D-Glc*p*-(1 → 3

Oligosaccharide	Spectrum	Atom[a]	H	G	F	E	D	C	B	A
OS(6)	ROESY	H-1				A 4[b] E 2 D 2	A 6_b A 6_a D 3 D 2 D 5	A 4 C 3 C 2	A 3 B 3 B 5	K 5 K 7 A 2
OS(7)	ROESY	H-1			F 2 C 2	A 4 E 2 D 2	A 6_b A 6_a D 3 D 2	A 3 C 3 C 5 C 2	A 3 B 3 B 5	K 5 K 7 A 2
OS(9)	NOESY	H-1	H 5[c] (m)[d] E 4 (s) H 3 (m) H 2 (w)	G 5[c] (m) F 4 (s) G 3 (m) G 2 (w)	F 2 (m) C 2 (m)	E 2 (m) D 2 (m)	A 6_b (w) A 6_a (w) D 3 (m) D 2 (w) D 5 (m)	A 3 (m) A 4 (w) C 3 (m) C 5 (m) C 2 (m)	A 3 (w) B 3 (m) B 5 (m) B 2 (w)	K 5 (s) K 7 (w) A 2 (m)
	HMBC	C-1	E 4 H 2	F 4 G 2	C 2	D 2	D 2	A 4	A 3 B 2	K 5
	HMBC	H-1	E 4 H 3 H 2	F 4 G 3 G 2	C 2 F 3 F 5	D 2 E 3 E 5	A 6	A 4	A 3[c]	A 3 K 5 A 5

Oligosaccharide	Spectrum	Atom[a]	Residue I	H	G	F	E	D	C	B	A	K
OS(10)	NOESY	H-1	**H** 4 (s) **I** 2 (s)	**H** 5 (w) **H** 3 (m) **E** 4 (m) **H** 2 (w)	**G** 5 (m) **F** 4 (m) **G** 3 (m) **G** 2 (w)	F 2 (s) C 2 (s)	**A** 4 (m) **E** 2 (s) **D** 2 (s)	**A** 6_b (s) **A** 6_a (s) **D** 3 (s) **D** 2 (m) **D** 5 (m)	**E** 1 (w) **B** 1 (w) **A** 3 (s) **A** 4 (m) **C** 3 (m) **C** 5 (m) **C** 2 (m)	**A** 3 (s) **B** 3 (m) **B** 5 (m) **B** 2 (w)	**K** 5 (s) **K** 7 (m) A 2 (s)	
	HMBC	C-1	**H** 4	**E** 4 **H** 2	**G** 5 **F** 4 **G** 2	C 2	**D** 2	**D** 2 **D** 5	**A** 4 **C** 5 **C** 2	**A** 3 **B** 5 **B** 2	**K** 5	
	HMBC	H-1	**H** 4 **I** 5 **I** 3	**E** 4	**F** 4	F 3 F 5	**E** 3 **E** 5	**A** 6		**A** 3[e]	**A** 3[f] **K** 5[f]	

[a] Atom from which correlations were observed.

[b] The notation should be interpreted as follows: H-1 in residue **E** has an intra-residue NOE correlation to H-2, and inter-residue NOE correlations to H-4 in residue **A** and H-2 in residue **D**, etc.

[c] The anomeric NMR signals for residues **G** and **H** are overlapping.

[d] The intensities of the NOE correlations in the NOESY spectra are given in parentheses: (w) indicates weak, (m) medium, and (s) strong correlations.

[e] Signals for **B** C-3 and **B** C-5 have chemical shifts close to **A** C-3.

[f] Signals for ^{13}C atoms are overlapping.

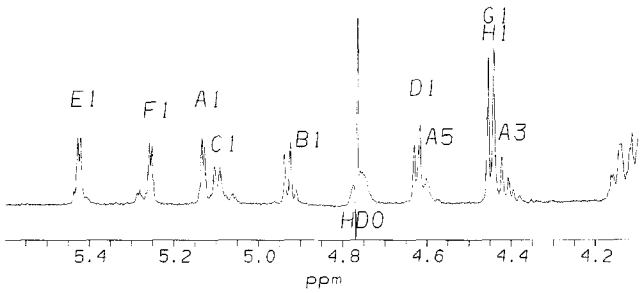

Fig. 2. ^{1}H NMR spectrum of OS(9) recorded at 600 MHz and 25 °C. Signals are annotated with residue designations and atom numbers.

had a correlation to H-5 in **K**. A correlation from H-1 in residue **A** was observed to a carbon resonating at $\delta \sim 76$. This signal could not be unambiguously assigned since both C-5 of **K** and C-3 of **A**, which are potential candidates for three-bond correlations, resonate in this region.

Structure of OS(9).—The δ 4.2–5.6 region of the ^{1}H NMR spectrum of OS(9) showed signals for eight anomeric protons and for two ring protons (Fig. 2). The hexosyl residues were designated **A**–**H**, and the Kdo residue was designated **K**. Residues **A** to **G** and residue **K** were assigned as sugar residues corresponding to those in OS(10), that is, to a 3,4,6-trisubstituted α-D-glucopyranosyl residue (**A**, $\delta_{H\text{-}1}$ 5.15), a β-D-glucopyranosyl group (**B**, $\delta_{H\text{-}1}$ 4.96), two 2-substituted β-D-glucopyranosyl residues (**C** and **D**, $\delta_{H\text{-}1}$ 5.12 and 4.65, respectively), two 4-substituted β-D-glucopyranosyl residues (**E** and **F**, $\delta_{H\text{-}1}$ 5.44 and 5.28, respectively), a β-D-galactopyranosyl group (**G**, $\delta_{H\text{-}1}$ 4.47), and one 5-substituted 3-deoxy-D-*manno*-octulopyranosonic acid (**K**). Residue **H** in OS(9) is assigned to a β-D-galactopyranosyl group ($\delta_{H\text{-}1}$ 4.47). Chemical shift data are given in Table 1.

Two trisaccharide branches, **G**-**F**-**C** and **H**-**E**-**D**, were established from inter-residue NOE data (Table 2). Thus, correlations between the anomeric proton and the proton on the linkage carbon were observed for all four disaccharide elements **G**-**F** (δ 4.47–δ 3.70), **F**-**C** (δ 5.28–δ 3.44), **H**-**E** (δ 4.47–δ 3.69), and **E**-**D** (δ 5.44–δ 3.48). Correlations to the branch-point residue were observed for the anomeric protons of residues **D**, **C**, and **B** to protons H-6 (both, δ 4.04 and 4.17), H-3 and H-4 (δ 4.44 and 4.03), and H-3 (δ 4.44), respectively. As in OS(10), residue **C** had the strongest NOE correlation between H-1 and H-3 of residue **A** and a weaker one between H-1 and H-4 in **A**. The anomeric proton of the branch-point residue **A** had NOE to H-5 and H-7 in Kdo, as observed also for OS(10). Thus, structure **9** was concluded for OS(9).

Inter-residue long-range heteronuclear correlations corroborating structure **9** were observed in an HMBC spectrum (Table 2). Correlations were observed between the overlapping signals of the anomeric carbons of residues **G** and **H** (both at δ 103.9) and the signals for H-4 of residues **F** (δ 3.70) and **E** (δ 3.69). The signal for the anomeric carbon of residue **E** (δ 97.7) had a correlation to H-2 of residue **D** (δ 3.48) and the anomeric carbon of residue **F** (δ 99.4) had a correlation to H-2 of residue **C** (δ 3.44). The signals for the anomeric protons of residues **H** and **G** (both at δ 4.47) had correlations to the C-4 signals for residues **E** and **F** (both at δ 79.1). The anomeric

protons of residues **E** (δ 5.44) and **F** (δ 5.28) had correlations to C-2 in residues **D** (δ 77.4) and **C** (δ 80.4), respectively. Thus, the structures of the two trisaccharide branches, **G-F-C** and **H-E-D**, established by NOE correlations were corroborated. The substitution pattern at residue **A**, the 3,4,6-trisubstituted α-D-glucopyranosyl residue, was demonstrated by the correlations from C-3 (δ 76.4), C-4 (δ 74.5), and C-6 (δ 68.7) in residue **A** to the anomeric protons of residues **B** (δ 4.96), **C** (δ 5.12), and **D** (δ 4.65), respectively. Correlations between the C-1 atoms of residues **B** and **C** were observed to the signals assigned to H-3 (δ 4.44) and H-4 (δ 4.03) of residue **A**, respectively. Finally, the observation of heteronuclear correlations between the signals for H-1 and C-1 of residue **A** (δ_H 5.15 and δ_C 100.3) and the signals for C-5 and H-5 of residue **K** (δ_C 76.1 and δ_H 4.08) corroborated structure **9**.

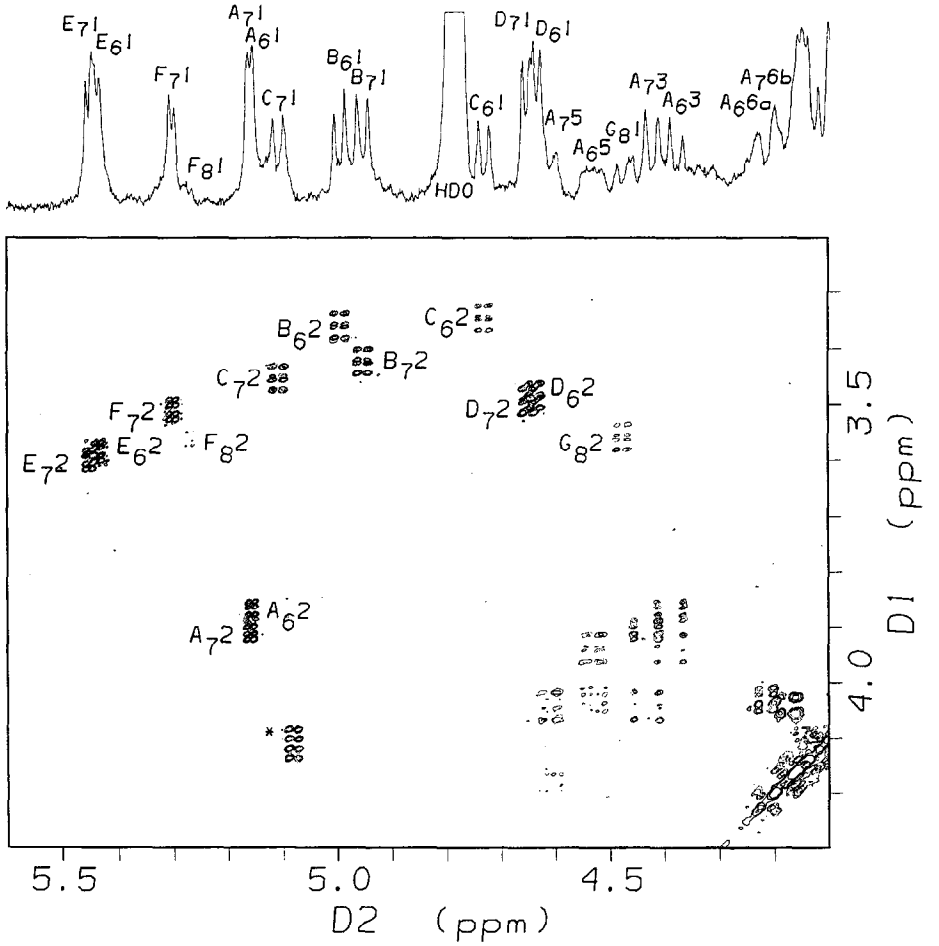

Fig. 3. Section of a phase-sensitive 2D double quantum filtered COSY spectrum of a mixture of OS(6), OS(7), and OS(8) recorded at 400 MHz and 25 °C. Cross-peaks are annotated along the D1 axis with residue designations and atom numbers.

Structures of OS(6), OS(7), and OS(8).—FABMS indicated that a hexa- and a hepta-saccharide were the main components of **f1**. This was also observed from the intensities of the cross-peaks in a double quantum filter COSY spectrum (Fig. 3) which suggested a slightly higher content of OS(7). Both the FAB mass spectrum and the COSY spectrum showed signals of low intensity that indicated the presence of an octasaccharide. The ^{1}H NMR signals (Table 1) from the COSY spectrum were assigned to residues designated **A-E** for OS(6) and **A-F** for OS(7). Signals corresponding to a residue designated **G** were observed for OS(8). Signals for a 5-substituted Kdo residue were observed, but the signals for the Kdo residues of the different oligosaccharides could not be distinguished. Further assignments of the ^{1}H NMR signals were made by analysis of HOHAHA spectra.

For the hexasaccharide, OS(6), residue **A** (δ_{H-1} 5.16) was assigned to a 3,4,6-trisubstituted α-D-glucopyranosyl residue, **B** (δ_{H-1} 4.99) and **C** (δ_{H-1} 4.73) to β-D-glucopyranosyl groups, **D** (δ_{H-1} 4.64) to a 2-substituted β-D-glucopyranosyl residue, and **E** (δ_{H-1} 5.44) to an α-D-glucopyranosyl group (Table 1). The following inter-residue NOE correlations (Table 2), in accordance with disaccharide elements, were observed in a ROESY spectrum (Fig. 4) δ 4.99–δ 4.39 (**B-A**), δ 4.73–δ 3.94 (**C-A**), δ 4.64–δ 4.21 and 4.03 (**D-A**), and finally for δ 5.44–δ 3.48 (**E-D**). Inter-residue NOE correlations between the branch-point residue and two signals at δ 4.08 (**K**, H-5) and 4.05 (**K**, probably H-7) demonstrated, as in the case of OS(9) and OS(10), residue **A** to substitute the 5-position of a Kdo residue. Thus, structure **6** is proposed for OS(6).

For the heptasaccharide, OS(7), residue **A** (δ_{H-1} 5.16) was assigned to a 3,4,6-trisubstituted α-D-glucopyranosyl residue, **B** (δ_{H-1} 4.95) to a β-D-glucopyranosyl group, **C** (δ_{H-1} 5.11) and **D** (δ_{H-1} 4.65) to 2-substituted β-D-glucopyranosyl residues, and **E** (δ_{H-1} 5.45) and **F** (δ_{H-1} 5.30) to α-D-glucopyranosyl groups (Table 1).

Inter-residue NOE correlations were observed in the ROESY spectrum (Table 2) corresponding to the following pairs of disaccharides δ 4.65–δ 4.18 and 4.04 (**D-A**), δ 5.45–δ 3.48 (**E-D**). Both **B** (δ 4.95) and **C** (δ 5.11) correlated to H-3 in **A** (δ 4.43) but from arguments given above this should no doubt correspond to elements **B**-(1 → 3)-**A**, and **C**-(1 → 4)-**A** (Table 2). A correlation δ 5.30–δ 3.45 demonstrates that a new element is present, **F**-**C**, and similarly to correlations in OS(6), residue **A** was shown to be linked to residue **K**. Thus, structure **7** is proposed for OS(7).

The content of OS(8) in **f1** was low as observed both from the FAB mass spectrum and from its appearance in the NMR spectrum. Only two weak cross-peaks, for H-1, H-2 of what are proposed to be residues **F** (δ_{H-1} 5.27, δ_{H-2} 3.56) and **G** (δ_{H-1} 4.47, δ_{H-2} 3.55), were observed for OS(8). The ^{1}H NMR signals for residues **A**–**E** and **K** of the octasaccharide presumably overlapped those of the corresponding residues of OS(7); hence, these residues are assumed to constitute the same hexasaccharide structural element as the corresponding residues do in OS(7). Residue **F** was assigned to a 4-substituted α-D-glucopyranosyl residue since the chemical shifts of the signals for H-1 and H-2 (δ 5.28 and δ 3.56, respectively) were in agreement with the corresponding chemical shifts for **F** (and not **E**) in OS(9) and OS(10) (δ_{H-1} 5.28 and δ_{H-2} 3.56). However, it could not be excluded that the eighth residue in OS(8) terminates the chain of sugars substituting the 6-position of the branch-point residue instead of the 4-position. Other ^{1}H NMR signals could not be observed in the HOHAHA spectra for the last

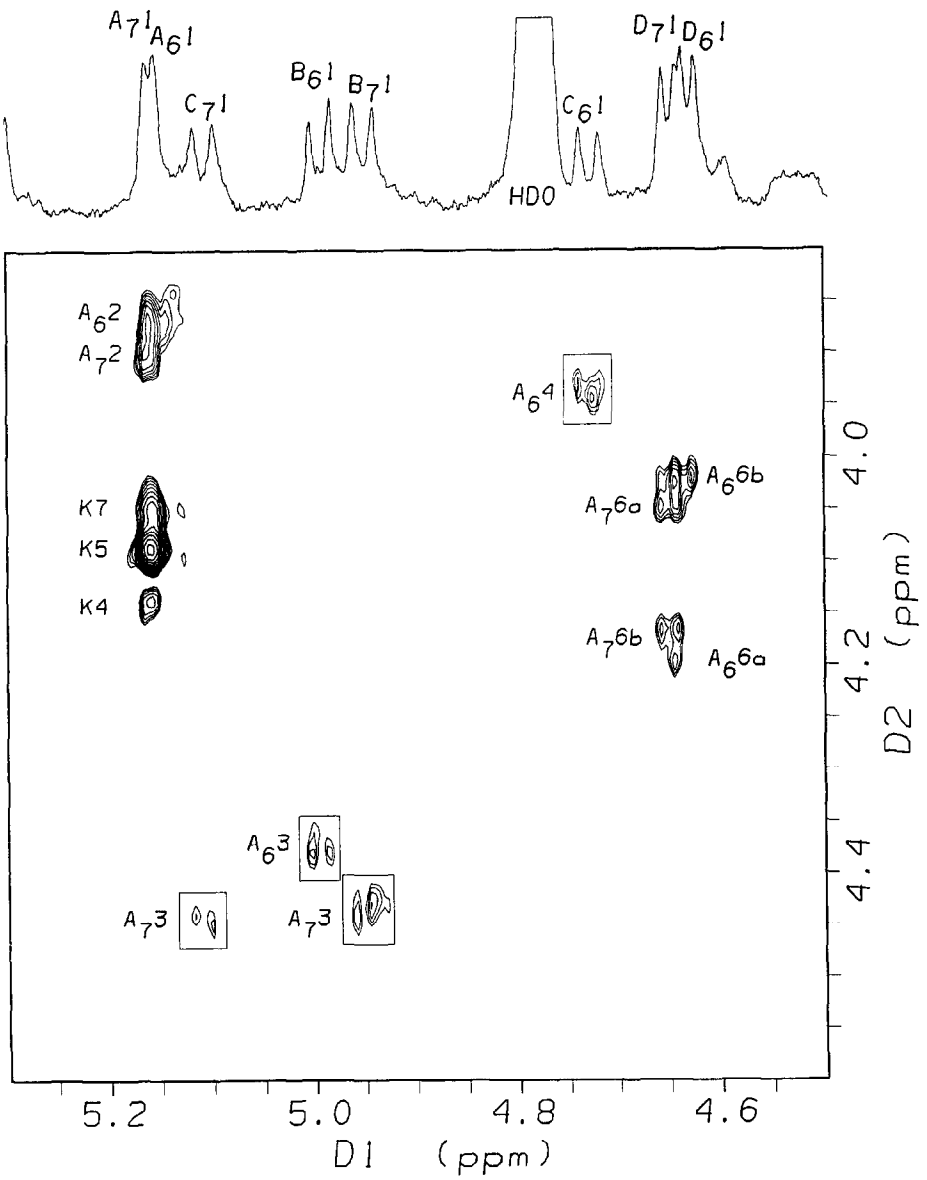

Fig. 4. Section of a phase-sensitive 2D ROESY spectrum of OS(6), OS(7), and OS(8) with a mixing time of 350 ms recorded at 500 MHz and 25 °C. Cross-peaks are annotated along the D2 axis with residue designations and atom numbers.

residue in OS(8), probably because of the small amount present. From the combined data structure **8** is proposed for OS(8).

Structure of OS(11).—The ^{1}H NMR spectrum of **f4**, which from FABMS analysis was demonstrated to contain an undecasaccharide, showed, in the region δ 4.2–5.6,

signals for nine anomeric protons and three ring protons. The signals were observed at chemical shifts that were identical to those of OS(10). Furthermore, two-dimensional $^1H,^1H$-correlated NMR spectra indicated that the spin systems present corresponded to those in OS(10). However, the signals for H-1 of residue **H** and H-1 and H-5 of residue **I** were more intense than in the ^1H NMR spectrum of OS(10). This may indicate the presence of two 4-*O*-α-D-galactopyranosyl-D-galactopyranosyl disaccharide elements, that is, OS(11) may have structure **11**. Although less intense than in the ^1H NMR spectrum of OS(10) the presence of a signal at δ 4.48 indicates a terminal β-D-Galp group not present in structure **11**. It is therefore suggested that another undecasaccharide of unknown structure is also present. Another possibility is that OS(10) is present despite the FAB mass spectrum of **f4**.

3. Conclusions

A comparison of the oligosaccharide structures of the three serotypes of *M. catarrhalis* provides a basis for prediction of the serotype-specific epitopes. Differences in structure are mainly limited to the 4-linked branch, which displays a terminal α-Glc*p*NAc-(1 → 2)-β-Glc*p*-(1 → 4 epitope specific for serotype A, a β-Gal*p*-(1 → 4)-α-Glc*p*-(1 → 2)-β-Glc*p*-(1 → 4 epitope specific for serotype B, and a β-Gal*p*-(1 → 4)-α-Glc*p*NAc-(1 → 2)-β-Glc*p*-(1 → 4 epitope specific for serotype C. The 6-linked branch was identical in the predominating oligosaccharide of type C and the oligosaccharide of type A. In type B the decasaccharide had the same structure of the branch, but in the nonasaccharide the terminal α-Gal*p* was missing, as was also the case with the hexa- and hepta-saccharides of type C. In type C these were minor components, while in type B the nonasaccharide and the decasaccharide were present in equal amounts. The terminal trisaccharide, α-Gal*p*-(1 → 4)-β-Gal*p*-(1 → 2)-α-Glc*p*(1 → , of the 6-linked branch is also present in the LPSs from other Gram-negative non-enteric bacteria, such as *Haemophilus influenzae* and *Neisseria gonorrhoeae* [11]. It is also found in the terminal part of glycolipids on the surface of human mucous membranes of epithelial cells. The disaccharide determinant α-D-Gal*p*-(1 → 4)-β-D-Gal*p* of this trisaccharide has been implicated in the pathogenesis of two other bacterial species. The adhesin expressed by the pili (PapG) of uropathogenic *Escherichia coli* has been shown to bind to glycosphingolipids of the uroepithelium containing this determinant [12]. It is also the receptor in the intestinal epithelium for the toxin secreted by *Shigella shigae* [13]. The outer region of the C-specific epitope, β-D-Gal*p*-(1 → 4)-α-D-Glc*p*NAc is also present in *H. influenzae*, *N. gonorrhoeae*, and *N. meningitidis*. In this case a sialic acid group substitutes the disaccharide element at the β-D-Gal*p* residue [11]. The disaccharide is also present in the human blood group antigen precursor, nLC-4Cer [11]. These epitopes may provide a way for the bacteria to evade the immune response or may be important during colonization and early invasion [14]. The finding that oligosaccharides of different chain length were present in the LPS from serotype B as well as from type C is probably a consequence of the biosynthetic mechanism of the cell-wall components of the bacteria. Since polymerization of the oligosaccharides and their coupling to the lipid part occurs outside the cytoplasmic membrane, particular modes of biosynthesis are operating,

involving transport of activated monomers through the cytoplasmic membrane and the polymerization through the activities of a number of glycosyl transferases. Depending on growth rate and other environmental conditions the oligosaccharides of the LPS molecules may not be fully substituted. This substitution would probably alter the antigenic specificity. In serotype B, the major components were OS(9) and OS(10). The oligosaccharides of shorter chain lengths were present in small amounts, and would probably not have any influence on the serological properties of the LPS.

It can be noted that, in serotype B, the substitution pattern is similar to that in serotypes A and C, always with a monosaccharide branch substituting the 3-position of the branch-point residue.

4. Experimental

General methods.—Concentrations were performed by flushing with air, or under diminished pressure, at < 40 °C or at room temperature. For GLC, a Hewlett–Packard 5890 instrument fitted with a flame-ionization detector was used. GLC-MS (EI) was performed on a Hewlett–Packard 5970 MSD. Fractionation of alditol acetates and partially methylated alditol acetates was performed on an HP-5 capillary column using the temperature program 180 °C (1 min) → 250 °C at 3 °C/min. Gel permeation chromatography was performed on either a column (1.6×40 cm) of Superdex 30 (Pharmacia Biotech, Uppsala, Sweden) at a flow rate of 96 mL/h, or on a column (1.6×40 cm) of Bio-Gel P-2 Fine (Bio-Rad Laboratories, Richmond, CA, USA) at a flow rate of 20 mL/h. Aqueous 0.07 M pyridinium acetate buffer of pH 5.4 was used as irrigant which was monitored with a differential refractometer (Waters R 403).

Bacteria and cultivation.—*Moraxella catarrhalis* strain CCUG 3292, which is representative for serotype B [15,16], was obtained from the culture collection at the University of Gothenburg. Bacterial cultures used for the production of LPS were grown in brain heart infusion broth (Difco Laboratories, Detroit, Michigan, USA) supplemented with 0.5% (w/v) yeast extract. A 50-L fermentor containing 30 L of medium was inoculated with 5 L of a late logarithmic phase culture. Agitation was maintained at 300 rpm and aeration at 10 L/min during growth. Bacteria were grown at a constant pH of 7.2 to late logarithmic phase, treated with formaldehyde to a final concentration of 1%, and kept overnight at 4 °C. The cells were harvested by centrifugation, washed once with PBS, suspended in H_2O, and lyophilized.

Preparation of LPS.—LPS was extracted from lyophilized bacteria, using phenol–$CHCl_3$–petroleum ether, as described by Galanos et al. [17] with the following modification. The LPS was precipitated by six volumes of 1:5 diethyl ether–acetone [18]. No significant amount of protein or nucleic acid was found in the LPS.

Isolation of OS.—The lipopolysaccharide preparation (190 mg) was suspended in aqueous 0.1 M NaOAc (20 mL) containing 0.1% SDS and was stirred for 5 min. Glacial acetic acid was added to pH 4.4 and the solution was kept at 100 °C for 2 h [19,20]. After lyophilization, the material was washed three times with ethanol, suspended in water, and centrifuged. The supernatant solution was then applied to a Sep-Pak C-18 cartridge, and was eluted with water. The eluate was lyophilized and purified by gel

permeation chromatography using a Superdex 30 column to yield an oligosaccharide-containing fraction, eluting at approximately 1.9 void volumes. The oligosaccharides were fractionated by high-performance anion-exchange chromatography on a CarboPac PA1 column using a Dionex system fitted with a pulsed amperometric detector. The samples were eluted at a flow rate of 4 mL/min with a gradient starting at 97% of eluent A (500 mM NaOH) and 3% of eluent B (aqueous 500 mM NaOH and 750 mM NaOAc solution), and ending after 30 min at 85% of eluent A and 15% of eluent B. Four fractions were collected, which were neutralized by addition of glacial AcOH, lyophilized, and desalted first on a Bio-Gel P-2 column and secondly on a Superdex 30 column to yield the preparations **f1** (< 1 mg), **f2** (4.1 mg), **f3** (4.2 mg), and **f4** (1.2 mg).

Sugar and methylation analysis.—A solution of the oligosaccharide mixture (0.1 mg) in 2 M CF_3CO_2H (0.5 mL) was kept at 120 °C for 3 h. The sugars in the hydrolysate were then converted into alditol acetates by conventional methods. Methylation analyses were performed using a modification of the NaOH method [21,22]. The oligosaccharide mixture (0.2 mg) was dissolved in dimethyl sulfoxide (50 μL) and methylated by sequential addition of an NaOH slurry in dimethyl sulfoxide (120 mg/mL, 50 μL; 20 min) and three additions of MeI (10, 10, and 20 μL) at 10-min intervals. The methylated glycans were recovered in the organic phase after partition between $CHCl_3$ (0.5 mL × 3) and M $Na_2S_2O_3$ (1 mL). The permethylated products were further purified by reversed-phase chromatography on a Sep-Pak C-18 cartridge [23].

Fast atom bombardment mass spectrometry.—A JEOL SX102 instrument was used for the FABMS experiments. The instrument was calibrated with CsI at a scan speed of 30 s and a mass range of *m/z* 0–2400. Ions were produced by a beam of Xe atoms (6 keV). A matrix of 3-nitrobenzyl alcohol was used for production of ions in the negative ion mode and a matrix of a 1:1 mixture of glycerol and thioglycerol was used in the positive ion mode.

NMR spectroscopy.—Spectra were recorded on JEOL Alpha 400 MHz and Varian Unity 500 and 600 MHz spectrometers using standard pulse sequences. NMR data were processed using standard JEOL and Varian software, or using Felix Version 2.3 (Biosym Technologies, Inc., USA). Samples were lyophilized twice with D_2O before they were redissolved in D_2O (99.96%). All spectra were recorded at 25 °C without spinning the sample. The signal arising from residual HDO was suppressed by presaturation. Chemical shifts are reported in ppm, using sodium 4,4-dimethyl-4-sila(2,2,3,3-$^2H_4$)pentanoate (TSP) (δ_H 0.00) or dioxane (δ_C 67.40) as internal reference. Reported ^{1}H NMR chemical shifts and $^3J_{H,H}$ values were obtained from one-dimensional spectra where possible, otherwise from the two-dimensional spectra. Reported ^{13}C NMR chemical shifts were obtained from ^{1}H-detected ^{1}H,^{13}C-correlated spectra. All two-dimensional spectra were recorded in the phase-sensitive mode. The spectra were multiplied by phase-shifted ($\pi/4$) sine-bell or square sine-bell functions and zero-filled to 2 × 2 K matrices prior to Fourier transformation.

The DQF COSY and HOHAHA spectra were recorded at 400 MHz with a recycle delay of 1.2 s between scans. The digital resolution was set to 0.71 Hz in F_2 and to 5.66 Hz in F_1. The spectra were zero-filled in F_1 to yield a digital resolution of 0.71 Hz. For measurement of the HOHAHA spectra the duration of the MLEV17 spin-lock, including two trim-pulses (2.5 μs), was set to 30, 60, and 90 ms. The NOESY spectra were

recorded at 600 MHz with a recycle delay of 3.0 s between scans. The digital resolution was set to 2.44 Hz in F_2 and to 9.77 Hz in F_1. The spectra were zero-filled in F_1 to yield a digital resolution of 2.44 Hz. The mixing time was set to 350 ms, and the observed NOE correlations were negative. The decoupled HSQC and HSQC-HOHAHA spectra were recorded at 400 MHz with a recycle delay of 1.2 s between scans. The digital resolution was set to 4.30 Hz in F_2 and to 31.4 Hz in F_1. The spectra were zero-filled to yield a digital resolution of 1.07 Hz in F_2 and 2.94 Hz in F_1. For measurement of the HSQC-HOHAHA spectra the duration of the spin-lock, including two trim-pulses (2.5 μs), was set to 30 ms. The HMQC spectra were recorded at 600 MHz with decoupling of the ^{13}C resonances. The recycle delay between scans was set to 1.8 s and the delay for coherence transfer was set to 3.33 ms $[1/(2 \times {}^{1}J_{C,H})]$. The digital resolution was set to 2.44 Hz in F_2 and to 109 Hz in F_1. The spectra were zero-filled to yield a digital resolution of 2.44 Hz in F_2 and 6.83 Hz in F_1.

The HMBC spectra were recorded at 600 MHz. The recycle delay between scans was set to 1.8 s, and the delays for coherence transfer were set to 3.33 ms $[1/(2 \times {}^{1}J_{C,H})]$ and 60 ms $[1/(2 \times {}^{n}J_{C,H})]$. The digital resolution was set to 2.44 Hz in F_2 and to 146 Hz in F_1. The spectra were zero-filled to yield a digital resolution of 2.44 Hz in F_2 and 6.83 Hz in F_1.

Acknowledgements

This work was supported by grants from the Swedish Research Council for Engineering Sciences, the Swedish Natural Science Research Council, and the Swedish Medical Research Council. We thank the Swedish Institute and the Wenner-Gren Centre foundation for fellowships to a member of the group (MR), and the Swedish NMR Centre for putting 500- and 600-MHz NMR facilities at our disposal.

References

[1] B.W. Catlin, *Clin. Microbiol. Rev.*, 3 (1990) 293–320.
[2] C.D. Marchant, *Am. J. Med.*, 88 (1990) 15–19.
[3] G.V. Doern, *Diagn. Microbiol. Infect. Dis.*, 4 (1986) 191–201.
[4] P.J. Hitchcock, L. Leive, P.H. Mäkelä, E.T. Rietschel, W. Strittmatter, and D.C. Morrison, *J. Bacteriol.*, 166 (1986) 699–705.
[5] J. Storm Fomsgaard, A. Fomsgaard, N. Høiby, B. Bruun, and C. Galanos, *Infect. Immun.*, 59 (1991) 3346–3349.
[6] M. Vaneechoutte, G. Verschraegen, G. Claeys, and A.-M. van den Abeele, *J. Clin. Microbiol.*, 28 (1990) 182–187.
[7] H. Masoud, M.B. Perry, and J.C. Richards, *Eur. J. Biochem.*, 220 (1994) 209–216.
[8] P. Edebrink, P.-E. Jansson, M.M. Rahman, G. Widmalm, T. Holme, M. Rahman, and A. Weintraub, *Carbohydr. Res.*, 257 (1994) 269–284.
[9] H. Masoud, M.B. Perry, J.R. Brisson, D. Uhrin, and J.C. Richards, *Can. J. Chem.*, 72 (1994) 1466–1477.
[10] P. Edebrink, P.-E. Jansson, M. Rahman, G. Widmalm, T. Holme, and M. Rahman, *Carbohydr. Res.*, 266 (1995) 237–261.
[11] R.E. Mandrell, J.M. Griffiss, and B.A. Macher, *J. Exp. Med.*, 168 (1988) 107–126.

[12] B. Lund, F.B. Lindberg, B. Marklund, and S. Normark, *Mol. Microbiol.*, 84 (1987) 5898–5902.
[13] J.E. Brown, P. Echeverria, and A.A. Lindberg, *Rev. Inf. Dis.*, 13 (1991) 298–303.
[14] J.N. Weiser, *Microb. Pathogen.*, 13 (1992) 335–342.
[15] I. Jönsson, T. Holme, A. Krook, M. Rahman, and M. Thorén, *Eur. J. Clin. Microbiol. Infect. Dis.*, 11 (1992) 919–922.
[16] M. Rahman and T. Holme, *J. Med. Microbiol.*, 44 (1996) 1–7.
[17] C. Galanos and M.A. Freudenberg, *Mediat. Inflamm.*, 2 (1993) S11–S16.
[18] N. Qureshi, K. Takayama, and E. Ribi, *J. Biol. Chem.*, 19 (1982) 11808–11815.
[19] M. Caroff, A. Tacken, and L. Szabó, *Carbohydr. Res.*, 175 (1988) 273–282.
[20] O. Holst, E. Röhrscheidt-Andrzejewski, H.-P. Cordes, and H. Brade, *Carbohydr. Res.*, 188 (1989) 213–218.
[21] M.J. McConville, S.W. Homans, J.E. Thomas-Oates, A. Dell, and A. Bacic, *J. Biol. Chem.*, 265 (1990) 7385–7390.
[22] I. Ciucanu and F. Kerek, *Carbohydr. Res.*, 131 (1984) 209–217.
[23] T.J. Waeghe, A.G. Darvill, M. McNeill, and P. Albersheim, *Carbohydr. Res.*, 123 (1983) 281–304.